

Study on quantitative parameters of intravoxel incoherent motion-diffusion weighted imaging to evaluate the treatment effect of transcatheter arterial chemoembolization combined with 3-dimensional conformal radiation therapy in patients with primary liver cancer

Z. Wu^{1*}, Y. Pang¹, J. Wang¹, P. Gao², W. Yin³, Y. Xia^{4*}

¹Department of Radiology, The Second People's Hospital of Hunan Province, Changsha, Hunan, China

²Department of Interventional Medicine, The Second People's Hospital of Hunan Province, Changsha, Hunan, China

³Department of Oncology, The Second People's Hospital of Hunan Province, Changsha, Hunan, China

⁴Medical Imaging Center, Jiujiang NO.1 People's Hospital, Jiujiang, Jiangxi, China

ABSTRACT

► Original article

*Corresponding author:

Yun Xia, M.D.,

E-mail:

yizherenx5555@163.com

Received: July 2025

Final revised: September 2025

Accepted: September 2025

Int. J. Radiat. Res., January 2026;
24(1): 97-102

DOI: 10.61186/ijrr.24.1.15

Keywords: Hepatocellular carcinomas; multiparametric magnetic resonance imaging, radiotherapy, chemoembolization therapeutic, ROC Curve.

Background: To observe the effect of quantitative parameters of intravoxel incoherent motion-diffusion weighted imaging (IVIM-DWI) in the evaluation of transcatheter arterial chemoembolization (TACE) combined with 3-dimensional conformal radiation therapy (3D-CRT) treatment effect. **Materials and Methods:** Research subjects were selected from 80 cases of patients with primary liver cancer (PLC) from May 2021 to October 2022. According to the judgment criteria of treatment effect of solid tumors, the patients were divided into complete remission (CR)/partial remission (PR) group (n=37) and stable disease (SD)/progressive disease (PD) group (n=43) after TACE combined with 3D-CRT treatment. The quantitative parameters of IVIM-DWI [F value, D* value, D value and apparent diffusion coefficient (ADC) value] in the two groups were compared. **Results:** The value of D*, F, D and ADC of IVIM-DWI quantitative parameters in the SD/PD group were all higher (P<0.05). The receiver operating characteristic (ROC) curve indicated that the area under curve (AUC) of the value of D*, F, D and ADC in IVIM-DWI quantitative parameters of patients with PLC to predict the effect of TACE combined with 3D-CRT in patients were 0.827, 0.777, 0.827, 0.863 and 0.923, and the AUC of the combination prediction was the largest. The sensitivity and specificity of combined prediction were 92.3% and 81.1% (Youden index 0.896), respectively. **Conclusion:** The value of D*, F, D and ADC in IVIM-DWI quantitative parameters are feasible to evaluate the treatment effect of TACE combined with 3D-CRT in patients with PLC.

INTRODUCTION

Transcatheter arterial chemoembolization (TACE) is the main approach of local minimally invasive surgery for primary liver cancer (PLC) patients at the present stage. By embolizing the local lesion vessels, we can cut off the nutrition and blood supply to the lesion, cause the ischemic necrosis of cancer cells, and control the disease progression⁽¹⁾. However, the efficacy of TACE alone is limited, which can easily lead to the recurrence and metastasis of residual tumor cells⁽²⁾. In order to further improve the therapeutic effect, 3 dimensional conformal radiation therapy (3D-CRT) can accurately locate and irradiate tumors and reduce the damage to the surrounding normal tissues, which has become an effective supplement for the treatment of PLC⁽³⁾. It is worth noting that patients with PLC are still at risk of recurrence after treatment because the tumor space cannot be completely filled with filler⁽⁴⁾. Therefore, it is necessary to study the treatment effect of TACE combined with 3D-CRT in patients with PLC to guide

advanced intervention and ensure the treatment effect of patients.

Diffusion weighted imaging (DWI) is a functional MRI, which reflects the biological information of tissue cells by detecting the degree of random movement restriction of water molecules in tissues. The signal strength of DWI is closely related to the irregular Brownian movement of water molecules in the block. However, it is also interfered by the blood flow of capillary network, so DWI signals cannot completely truly reflect the diffusion coefficient. Based on this, intravoxel incoherent motion-diffusion weighted imaging (IVIM-DWI) appears, which effectively makes up for the shortcomings of DWI, it is more applied in clinic⁽⁵⁾. True molecular diffusion (D) reflects tumor cell density, Pseudo-diffusion coefficient (D*) represents microcirculation perfusion, Perfusion fraction (F) associated angiogenesis - changes in these parameters can explain the tumor biological response to treatment⁽⁶⁾.

Although in recent years, studies have reported the advantages of IVIM-DWI in the evaluation of

microcirculation of liver cancer (7). However, relevant studies on IVIM-DWI evaluation of TACE combined with 3D-CRT treatment effect in patients with PLC are rare. This study is the first to apply IVIM-DWI quantitative parameters (D^* , F , D , ADC) to the efficacy evaluation system of TACE combined with 3D-CRT, and the predictive efficacy was confirmed by multi-parameter ROC analysis, which provides a new non-invasive imaging method for early efficacy judgment of combined treatment of PLC.

MATERIALS AND METHODS

General data

Based on the effect size of ADC value ($d=0.8$) in the pilot study ($n=20$), set $\alpha=0.05$ and $\beta=0.2$. GPower 3.1 calculated that 76 samples were needed, and 80 samples were included after considering the dropout rate. Research subjects are selected from 80 cases of patients with PLC from May 2021 to October 2022. All enrolled subjects met the following inclusion conditions: (1) Inclusion criteria: ① PLC was diagnosed according to the Standardization for diagnosis and treatment of hepatocellular carcinoma (2022 edition) and confirmed by pathology; ② All the enrolled subjects successfully underwent TACE combined with 3D-CRT treatment; ③ IVIM-DWI was performed in our hospital; ④ No extrahepatic metastasis is found according to pathological results, and tumors in other parts are excluded; ⑤ All of them were the first onset diseases; ⑥ The enrolled subjects signed the study consent. (2) Exclusion criteria: ① Subjects who are allergic to contrast agents; ② Patients with ascites; (3) Patients with respiratory diseases, unable to cooperate with the examination; ④ Accompanied with septic shock or bacteremia; ⑤ Patients with mental or psychological diseases could not cooperate with the research to develop smoothly. This study was approved by the Ethics committee of The Second People's Hospital of Hunan Province (No.2021-061-1;2021-6-15), and all study subjects signed an informed consent form.

Method

IVIM-DWI examination

Instrument: Achieva 3.0T TX magnetic resonance scanner manufactured (Ingenia CX, Philips, Netherlands). Examination time: 1d before treatment. Before the examination, the patient was guided to correct respiratory training, breath-holding transverse T1WI double echo sequence (scan sequence: TE: 2.9 ms, TR: 250 ms, Matrix 288×192, FOV: 34-38 cm, layer thickness/layer spacing: 6.0/0.6cm, scan 16-22s), transverse T2WI fat suppression sequence (scan sequence: TE: 100-130 ms, TR: 6000-70000 ms, Matrix 288×224, FOV 34-38 cm, layer thickness/layer spacing 6.0/0.6mm, layers 20-24), respiratory trigger lateral axis (scan

sequence: TE: 60.8 ms, TR: 3529 ms, Matrix 128×160, FOV 28×34 cm-32×40 cm, layer thickness/layer spacing 5.0/0.5mm). B Values of 0, 10, 20, 50, 100, 150, and 200s/mm² (2 acquisitions) and 400, 600, 800, 1000, and 1200s/mm² (3 acquisitions) were selected.

IVIM-DWI processing

The data obtained from IVIM-DWI examination were transmitted to the workstation for processing. Two radiologists independently delineated the Region of Interest (ROI) (avoiding the necrotic area), and the central slice of the lesion with diameter ≥ 1 cm was taken, and the results were averaged. A standard apparent diffusion coefficient (ADC) plot was obtained through analysis by monoexponential model and the ADC value was counted. D^* , D , and F was obtained using a biexponential model, and the region of interest was manually drawn. The above data are counted 3 times and averaged. figure 1 shows the results of IVIM-DWI for a given patient.

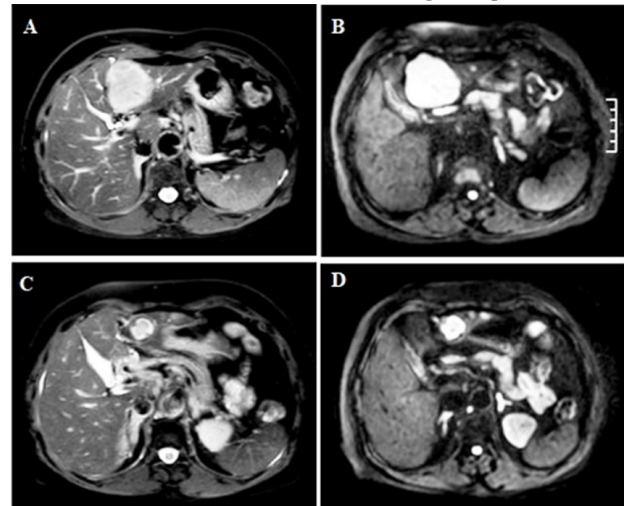


Figure 1. Male, 36 years old, IVIM-DWI findings. (A, B) Results of examination before treatment. T2WI axial view and D value distribution diagram. (C, D) Results of examination after treatment. T2WI axial view and D value distribution diagram. The tumor shrank significantly, and a small amount of iodine deposition was observed in the tumor.

TACE treatment

Selinger technique was used for percutaneous femoral artery puncture: The blood supply artery of the tumor was punctured after evaluation and assisted puncture by angiography technique, and the embolic drugs [fluorouracil injection 750mg/m²+oxaliplatin injection 50mg/m² (H31020593, Shanghai Xudong Haipu Pharmaceutical Co., LTD.)] were injected. Then all the supply vessels were embolized with the mixed emulsion [pirarubicin for injection 50mg/m²+lipiodol 5-15mL (H10930105, Shenzhen Wanle Pharmaceutical Co., LTD.)]. If arterial shunt was large, embolization was performed with gelatin sponge. 4w/times, three times for all patients.

3D-CRT treatment

3D-CRT was performed 2-3 weeks after completion of TACE. After the thermoplastic film was fixed and cooled, the patients underwent enhanced CT scanning and the images were uploaded to complete the radiotherapy plan design. The tumor target area was delineated, the possible organs involved were identified, and the planning target area was set. The planning target volume (PTV) was treated with linear accelerator. The prescribed dose standard was 5-10 Gy per time, 3 times per week for 3 weeks. The dose was adjusted according to the location of the tumor: 36-45Gy for the central type and 54-63Gy for the peripheral type, and 95% of the planning target volume (PTV) reached the prescribed dose during treatment.

Treatment effect evaluation and study grouping

Treatment effect was evaluated according to RECIST-New guidelines to evaluate the response to treatment in solid tumors⁽⁸⁾: Complete remission (CR): all target lesions disappeared and remained for at least 4w; Partial remission (PR): maximum diameter and reduction of target lesion $\geq 30\%$; Stable disease (SD): the maximum diameter and reduction of the target lesion is less than 30% or the increase is less than 20%; Progressive disease (PD): maximum diameter and increase in target lesion $\geq 20\%$. Patients were grouped according to RECIST at 4 weeks after treatment. CR and PR were defined as one group (CR/PR group) and SD and PD as one group (SD/PD group).

Quantitative Real-time polymerase chain reaction (qRT-PCR)

Fasting venous blood was collected from patients at 1 day before treatment, and total RNA was extracted using TRIzol reagent (Invitrogen, USA). The purity was verified by reverse transcription using PrimeScript RT Master Mix (TaKaRa, Japan) to obtain cDNA. Subsequently, PCR reactions were performed according to SYBR Green Master Mix (Applied Biosystems, USA) under 40 cycles of 95 ° C for 30s, 95 ° C for 5s, and 72 ° C for 30s. The primer sequences were constructed by design (table 1), and the expression of *p53*, *PTEN*, and *MYC* mRNA was calculated by the $2^{-\Delta\Delta Ct}$ method.

Table 1. Primer sequences.

	F (5'-3')	R (5'-3')	bp
<i>p53</i>	GGACGATATTGAACAA-GATGGAG	TCGTTTCTGAT-TCGTCCTGAA	128
<i>PTEN</i>	GCTGA-GATGCCTTCTTCTTG	CAGTTCCTTCTCCAC-TGTTC	112
<i>MYC</i>	CGGAGGAGACGCTGA-GAAAA	GCTGTTTCTTCTCAG-TCTC	105
<i>GAPDH</i>	GAAGGTGAAGGTCG-GAGTC	GAAGATGGTGATGGGAT-TTC	110

Statistical method

SPSS24.0 was used to process the data. Shapiro-Wilk test was used to test whether the measurement

data conformed to the normal distribution, " $\bar{x} \pm s$ " was used to indicate the measurement data conformed to the normal distribution, and *t* test was used to compare the independent samples between groups; "n(%)" is used to represent count data, and χ^2 test was used. and the rank data were tested using rank sum test. The receiver operating characteristic (ROC) curve of subjects was drawn, and the value of F, D*, D and ADC in IVIM-DWI quantitative parameters for predicting the TACE treatment effect in patients with PLC was tested, which was evaluated by the area under curve (AUC), predictive value details were shown in table 2. For combination prediction, Logistic regression coefficients were used to establish a joint formula, and then ROC was performed. With the test level $\alpha=0.05$.

Table 2. AUC predictive value details.

AUC	Predictive value
≤ 0.50	No
$0.50 < \text{AUC} \leq 0.70$	Low
$0.70 < \text{AUC} \leq 0.90$	Medium
> 0.90	High

Note: Area under curve (AUC).

RESULTS

Treatment effects

Among the 80 patients with PLC treated with TACE combined with 3D-CRT, 15 patients achieved CR, with a CR rate of 18.75% (15/80), 22 patients achieved PR, with a PR rate of 27.50% (22/80), and 37 cases were in the CR/PR group. 29 patients achieved SD, with a SD rate of 36.25% (29/80), 14 patients achieved PD, with a PD rate of 17.50% (14/80), and 43 cases in the SD/PD group.

Comparison of general data

There was no significant difference in age, gender, and Liver function Child-pugh classification between CR/PR group and SD/PD group ($P > 0.05$). Moreover, there were no significant differences in the mRNA levels of *p53*, *PTEN*, and *MYC* between the two groups ($P > 0.05$) (table 3 and figure 2).

Comparison of IVIM-DWI parameters

The value of D*, F, D and ADC of IVIM-DWI quantitative parameters in the SD/PD group were all lower ($P < 0.05$) (table 4).

Predictive treatment efficacy analysis of IVIM-DWI quantitative parameters

The value of D*, F, D and ADC in IVIM-DWI quantitative parameters for patients with PLC were taken as test variables, and the treatment effect of patients after TACE was taken as a dependent variable (1=SD/PD, 0=CR/PR). ROC curve was drawn (figure 3). The ROC curve indicated that the AUC of the value of D*, F, D and ADC of in IVIM-DWI quantitative parameters of patients with PLC to predict the effect of TACE in patients with TACE alone

and in combination were 0.827, 0.777, 0.827, 0.863 was the largest (table 5). and 0.923, and the AUC of the combination prediction

Table 3. Comparison of general data.

Factor		CR/PR group(n=37)	SD/PD group(n=43)	Statistical values	P
Gender	Male	20(54.05)	25(58.14)	$\chi^2=0.135$	0.713
	Female	17(45.95)	18(41.86)		
Age ($\bar{x}\pm s$, years)		58.11 \pm 2.85	58.51 \pm 2.77	$t=0.635$	0.527
Liver function Child-pugh classification ⁽⁹⁾	Grade A	23(62.16)	20(46.51)	$Z=1.391$	0.164
	Grade B	14(37.84)	23(53.49)		
BCLC stage ⁽¹⁰⁾	Stage B	18(48.65)	22(51.16)	$Z=0.223$	0.824
	Stage C	19(51.35)	21(48.83)		
	Stage III	20(54.05)	25(58.14)		
Tumor maximum diameter	<5cm	12(32.43)	15(34.88)	$\chi^2=0.053$	0.817
	\geq 5cm	25(67.57)	28(65.12)		
TNM ⁽¹¹⁾	Stage IV	17(45.95)	18(41.86)	$Z=0.365$	0.715
	Stage III	20(54.05)	25(58.14)		
Lesion location	Left lobe	10(27.03)	9(20.90)	$\chi^2=0.449$	0.799
	Right lobe	15(40.54)	18(41.86)		
	Left and right lobe	12(32.43)	16(37.21)		
ECOG score ⁽¹²⁾ ($\bar{x}\pm s$, score)		1.00 \pm 0.47	1.09 \pm 0.53	$t=0.798$	0.428
Karnofsky score ($\bar{x}\pm s$, score)		75.11 \pm 2.05	75.19 \pm 2.15	$t=0.170$	0.866

Note: Complete remission (CR), Partial remission (PR), Stable disease (SD), Progressive disease (PD), Barcelona (BCLC), Tumor node metastasis (TNM), Eastern Cooperative Oncology Group (ECOG).

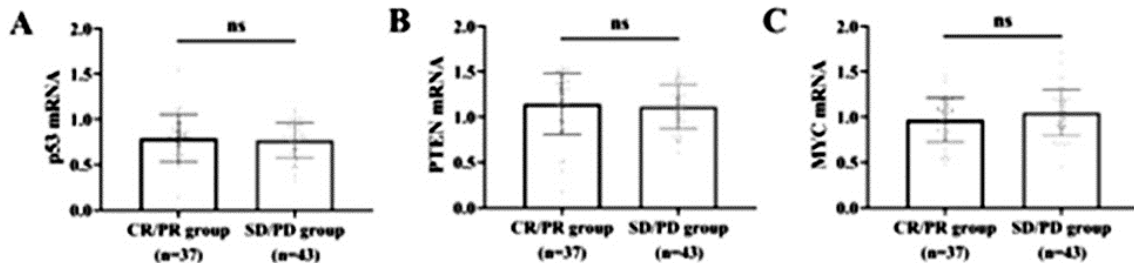


Figure 2. Comparison of PCR test results. (A) Comparison of p53 mRNA. (B) Comparison of PTEN mRNA. (C) Comparison of MYC mRNA. ns indicated that there was no significant difference between the two groups (P>0.05).

Table 4. Comparison of IVIM-DWI parameters.

	CR/PR group(n=37)	SD/PD group(n=43)	Statistical values	P
D value ($\bar{x}\pm s$, *10 ⁻³ mm ² /s)	1.10 \pm 0.30	1.80 \pm 0.45	$t=2.791$	0.007
D* value ($\bar{x}\pm s$, *10 ⁻³ mm ² /s)	19.30 \pm 6.12	25.25 \pm 9.30	$t=2.516$	0.014
F value ($\bar{x}\pm s$,%)	0.25 \pm 0.04	0.38 \pm 0.03	$t=16.577$	<0.001
ADC value ($\bar{x}\pm s$, *10 ⁻³ mm ² /s)	1.02 \pm 0.36	1.42 \pm 0.45	$t=4.341$	<0.001

Note: Complete remission (CR), Partial remission (PR), Stable disease (SD), Progressive disease (PD), Apparent diffusion coefficient (ADC), Pseudo-diffusion coefficient (D*), True molecular diffusion (D), Perfusion fraction (F).

Table 5. Efficacy analysis of IVIM-DWI quantitative parameters in predicting the treatment effect of TACE in patients with PLC.

Indicator	AUC	95%CI of AUC	Standard error	P	Cut-off value	Sensitivity	Specificity	Youden index
D value	0.827	0.732-0.962	0.033	<0.001	1.195	0.927	0.651	0.728
D* value	0.777	0.580-0.812	0.059	<0.001	8.085	0.777	0.819	0.826
F value	0.827	0.754-0.986	0.034	<0.001	0.215	0.927	0.438	0.815
ADC values	0.863	0.621-0.894	0.057	<0.001	0.650	0.863	0.746	0.856
Combination	0.923	0.823-0.987	0.024	<0.001	0.431	0.923	0.811	0.896

Note: Apparent diffusion coefficient (ADC), Pseudo-diffusion coefficient (D*), True molecular diffusion (D), Perfusion fraction (F), Area under curve (AUC), 95% confidence interval (95%CI).

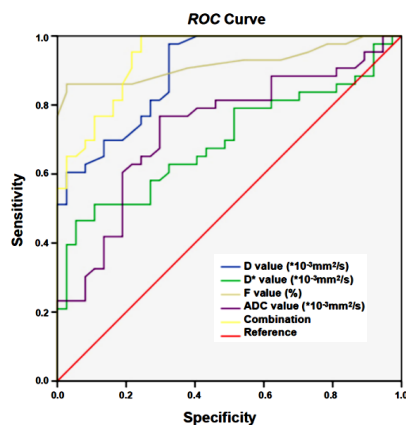


Figure 3. ROC curve of IVIM-DWI quantitative parameters predicting the effect of TACE treatment in patients with PLC.

DISCUSSION

IVIM-DWI distinguishes the blood perfusion in the capillary from the irregular movement of water molecules in the tissue, that means to separate the pseudo diffusion from the true diffusion of the tissue, and evaluate the perfusion and diffusion of the tissue respectively, which can truly reflect the blood supply status and cell tissue density of tumors, and then provide necessary quantitative information for clinical diagnosis⁽¹³⁾. IVIM-DWI obtains DWI images by collecting several B values. The value of D*, F, D and ADC of can be acquired according to the

biexponential model, where D value belongs to the true diffusion coefficient and is mainly related to the diffusion limitation of pure water molecules inside and outside of cells caused by macromolecules, cell membrane and fibers⁽¹⁴⁾. D* value belongs to pseudo diffusion coefficient, which is closely associated with the microcirculation perfusion of capillary network and reflects the capillary flow velocity of target tissue⁽¹⁵⁾. F value refers to the ratio of capillary volume in voxels to the volume of the whole tissue, which is related to the microvessel density in immature or normal capillaries and represents the angiogenesis speed to a certain extent. As it is the same as D* value, it all represents the microcirculation perfusion of capillaries. Therefore, the change trends of D* value and F value are consistent^(16,17). ADC value is the activity of IVIM-DWI monoexponential model, which has high value in the initial diagnosis of tumor, curative effect and prognosis evaluation, but ADC value cannot simply reflect the diffusion of water molecules in tissue, ADC value is also related to the blood perfusion effect of capillary network, and there is bias when it is used in clinic alone⁽¹⁸⁾. The results indicated that the value of D*, F, D and ADC of IVIM-DWI quantitative parameters in the SD/PD group were higher. Therefore, F value, D* value, D value and ADC value in IVIM-DWI quantitative parameters were considered for the evaluation of TACE combined with 3D-CRT treatment effect of PLC.

To verify the above hypothesis, the ROC curve drawn in the study indicated that the AUC of the value of D*, F, D and ADC of in the IVIM-DWI quantitative parameters of patients with PLC in predicting the treatment effect of TACE combined with 3D-CRT for patients was 0.923, suggesting that the IVIM-DWI quantitative parameters were valuable in predicting the treatment effect of TACE combined with 3D-CRT for patients with PLC. The possible reasons for analysis were as follows: ① After TACE combined with 3D-CRT treatment, patients with PLC who failed to respond to the treatment still had residual tumor tissues in their bodies, with high cell density of focal tissues, increased nucleus-to-mass ratio, blocked diffusion of water molecules, changes in capillary movement, and microcirculatory dysfunction. IVIM-DWI examination showed that the D* and F values were decreased⁽¹⁹⁾. ② The focal tissue was in a state of hypoxia-ischemia after TACE combined with 3D-CRT, and high local concentration of cytotoxicity increased the permeability of tumor cells while killing cancer cells, resulting in massive outflow of intracellular fluid, increased freedom of extracellular water molecules and accelerated diffusion movement. As a result, the D value and ADC value were increased in patients with effective treatment, but those with ineffective treatment showed that the diffusion of water molecules inside and outside the focal tissue could not achieve the above-mentioned phenomena, so the D value and

ADC value were small⁽²⁰⁾. In view of the above reasons, the treatment effect of TACE combined with 3D-CRT can be pre-evaluated in clinical practice by detecting the quantitative parameters of IVIM-DWI in patients, and it also indicates that after the pre-evaluation of the treatment effect, in-depth or combined interventions can be provided for patients with unsatisfactory efficacy for improving the treatment effect of patients with PLC and maximize the treatment benefit of patients.

It is worth noting that although the molecular pathogenesis theory has been the focus of research in recent years, *p53*, *PTEN*, and *MYC* are commonly used clinical objective tests for PLC. However, in this study, we found that there was no significant difference in the expression of *p53*, *PTEN* and *MYC* mRNA in patients with different response. This emphasizes that IVIM-DWI still has advantages in clinical application. Analysis of the reasons showed that although *p53*, *PTEN*, *MYC* and other genes have been confirmed and involved in the development of PLC, changes in drug resistance and immune microenvironment obviously have a greater impact on their expression levels⁽²¹⁻²³⁾. At the same time, because the baseline data of CR/PR group and SD/PD group were consistent, the pathological conditions of the patients in this study were relatively type.

This study has the following limitations: ① the small sample size of a single center (n=80) may affect the statistical power; ② IVIM parameters were not dynamically monitored during treatment; ③ Genetic analysis was limited to baseline level only; ④ RECIST criteria does not include the evaluation of necrosis rate, which may underestimate the value of imaging parameters. In the future, multi-center and large-sample studies are needed to integrate radiomics and temporal changes of gene expression in treatment.

In summary, the value of D*, F, D and ADC of IVIM-DWI quantitative parameters are feasible for the evaluation of TACE combined with 3D-CRT treatment effect in patients with PLC.

Ethical Approval: The study involving human subjects complied with the Declaration of Helsinki and was approved by the ethical committee of The Second People's Hospital of Hunan Province (No.2021-061-1;2021-6-15), and all participants provided written informed consent.

Conflicts of Interest: The authors report no conflict of interest.

Availability of data and materials: The data used to support the findings of this study are available from the corresponding author upon request.

Funding: Not applicable.

Author Contributions: ZH.W., designed the study; ZH.W. and YW.P., wrote and revised the main manuscript text, JJ.W. and PF.G., collected and analyzed data, W.Y., supervised the study. All authors reviewed and approved the final manuscript.

REFERENCES

1. Stallwood-Hall C, Anderson J, Ebeid A (2022) Systematic review and meta-analysis of arterial embolization compared with traditional management on outcomes of traumatic massive facial haemorrhage. *ANZ Journal of Surgery*, **92**(5): 988-993.
2. Chen W, Chiang CL, Dawson LA (2021) Efficacy and safety of radiotherapy for primary liver cancer. *Chinese Clinical Oncology*, **10**(1): 9.
3. Roberts HJ and Wo JY (2022) Stereotactic body radiation therapy for primary liver tumors: An effective liver-directed therapy in the toolbox. *Cancer*, **128**(5): 956-965.
4. Lissing M, Vassiliou D, Floderus Y, Harper P, Bottai M, Kotopoulou M, Hagström H, Sardh E, Wahlin S (2022) Risk of primary liver cancer in acute hepatic porphyria patients: A matched cohort study of 1244 individuals. *Journal of Internal Medicine*, **291**(6): 824-836.
5. Rauh SS, Riechinger AJ, Ohlmeyer S, Hammon M, Saake M, Stemmer A, Uder M, Hensel B, Laun FB (2020) A mixed waveform protocol for reduction of the cardiac motion artifact in black-blood diffusion-weighted imaging of the liver. *Magn Reson Imaging*, **67**: 59-68.
6. Yang C, Wei XQ, Zheng J, Tao YY, Gong XQ, Li L, Li ZM, Yang L, Mao Q, Zhou MT, Zhang XM (2023) A correlative study between IVIM-DWI parameters and VEGF and MMPs expression in hepatocellular carcinoma. *Quant Imaging Med Surg*, **13**(3): 1887-1898.
7. Zhou Y, Yang G, Gong XQ, Tao YY, Wang R, Zheng J, Yang C, Peng J, Yang L, Li JD, Zhang XM (2021) A study of the correlations between IVIM-DWI parameters and the histologic differentiation of hepatocellular carcinoma. *Scientific Reports*, **11**(1): 10392.
8. Seymour L, Bogaerts J, Perrone A, Ford R, Schwartz LH, Mandrekar S, Lin NU, Litière S, Dancey J, Chen A, Hodi FS, Therasse P, Hoekstra OS, Shankar LK, Wolchok JD, Ballinger M, Caramella C, de Vries EGE (2017) iRECIST: guidelines for response criteria for use in trials testing immunotherapeutics. *The Lancet. Oncology*, **18**(3): e143-e152.
9. Peng Y, Qi X, Guo X (2016) Child-Pugh versus MELD score for the assessment of prognosis in liver cirrhosis: A systematic review and meta-analysis of observational studies. *Medicine (Baltimore)*, **95**(8): e2877.
10. Furukawa K, Shiba H, Horiuchi T, Shirai Y, Haruki K, Fujiwara Y, Sakamoto T, Gocho T, Yanaga K (2017) Survival benefit of hepatic resection for hepatocellular carcinoma beyond the Barcelona Clinic Liver Cancer classification. *Journal of Hepato-Biliary-Pancreatic Sciences*, **24**(4): 199-205.
11. Wittekind C (2010) [2010 TNM system: on the 7th edition of TNM classification of malignant tumors]. *Der Pathologe*, **31**(5): 331-332.
12. Asbury RF, Lipsitz S, Graham D, Falkson CI, Baez L, Benson AB (2000) Treatment of squamous cell esophageal cancer with topotecan: an Eastern Cooperative Oncology Group Study (E2293). *American Journal of Clinical Oncology*, **23**(1): 45-46.
13. Yin Z, Li X, Zhang Y, Tao J, Yang Y, Fang S, Zhang Z, Yuan Y, Liu Y, Wang S (2022) Correlations between DWI, IVIM, and HIF-1 α expression based on MRI and pathology in a murine model of rhabdomyosarcoma. *Magn Reson Med*, **88**(2): 871-879.
14. Ni X, Wang W, Li X, Li Y, Chen J, Shi D, Wen J (2020) Utility of diffusion-weighted imaging for guiding clinical management of patients with kidney transplant: A prospective study. *J Magn Reson Imaging*, **52**(2): 565-574.
15. Zhang Y, Zhang K, Jia H, Xia B, Zang C, Liu Y, Qian L, Dong J (2022) IVIM-DWI and MRI-based radiomics in cervical cancer: Prediction of concurrent chemoradiotherapy sensitivity in combination with clinical prognostic factors. *Magn Reson Imaging*, **91**: 37-44.
16. Wang H, Zhu L, Li G, Zuo M, Ma X, Wang J (2020) Perfusion parameters of intravoxel incoherent motion based on tumor edge region of interest in cervical cancer: evaluation of differentiation and correlation with dynamic contrast-enhanced MRI. *Acta Radiol*, **61**(8): 1087-1095.
17. Meng N, Wang XJ, Sun J, Huang L, Wang Z, Wang KY, Wang J, Han DM, Wang MY (2020) Comparative study of amide proton transfer-weighted imaging and intravoxel incoherent motion imaging in breast cancer diagnosis and evaluation. *J Magn Reson Imaging*, **52**(4): 1175-1186.
18. Lei Y, Zhou J, Liu J, Xia X, Wang P, Peng Y, Xie X, Liao Y, Wan Q, Li X (2022) The CT and PET/CT findings in primary pulmonary lymphoepithelioma-like carcinoma with pathological correlation: a study of 215 cases. *Clinical Radiology*, **77**(3): e201-e207.
19. Zhang Z and Pedrycz W (2019) A consistency and consensus-based goal programming method for group decision-making with interval-valued intuitionistic multiplicative preference relations. *IEEE Transactions on Cybernetics*, **49**(10): 3640-3654.
20. Yang D, She H, Wang X, Yang Z, Wang Z (2020) Diagnostic accuracy of quantitative diffusion parameters in the pathological grading of hepatocellular carcinoma: A meta-analysis. *J Magn Reson Imaging*, **51**(5): 1581-1593.
21. Abe H, Yasunaga Y, Yamazawa S, Nakai Y, Gono W, Nishioka Y, Muroto K, Sasaki K, Arita J, Kawai K, Nozawa H, Hasegawa K, Ishihara S, Ushiku T (2022) Histological growth patterns of colorectal cancer liver metastases: a strong prognostic marker associated with invasive patterns of the primary tumor and p53 alteration. *Human Pathology*, **123**: 74-83.
22. Qian X, Cai J, Qi Q, Han J, Zhu X, Xia R, Zhang Q (2023) Preoperative fibrinogen is associated with the clinical survival of primary liver cancer patients and promotes hepatoma metastasis via the PTEN/AKT/mTOR pathway. *Heliyon*, **9**(6): e16696.
23. D'Artista L, Moschopoulou AA, Barozzi I, Craig AJ, Seehawer M, Herrmann L, Minnich M *et al.* (2023) MYC determines lineage commitment in KRAS-driven primary liver cancer development. *Journal of Hepatology*, **79**(1): 141-149.